ELSEVIER

Paramyxovirus membrane fusion: Lessons from the F and HN atomic structures

Robert A. Lamb [a,b,*], Reay G. Paterson [b], Theodore S. Jardetzky [b]

[a] Howard Hughes Medical Institute, Northwestern University, Evanston, IL 60208-3500, USA
[b] Department of Biochemistry, Molecular Biology and Cell Biology, Northwestern University, 2205 Tech Drive, Evanston, IL 60208-3500, USA

Abstract

Paramyxoviruses enter cells by fusion of their lipid envelope with the target cell plasma membrane. Fusion of the viral membrane with the plasma membrane allows entry of the viral genome into the cytoplasm. For paramyxoviruses, membrane fusion occurs at neutral pH, but the trigger mechanism that controls the viral entry machinery such that it occurs at the right time and in the right place remains to be elucidated. Two viral glycoproteins are key to the infection process—an attachment protein that varies among different paramyxoviruses and the fusion (F) protein, which is found in all paramyxoviruses. For many of the paramyxoviruses (parainfluenza viruses 1–5, mumps virus, Newcastle disease virus and others), the attachment protein is the hemagglutinin/neuraminidase (HN) protein. In the last 5 years, atomic structures of paramyxovirus F and HN proteins have been reported. The knowledge gained from these structures towards understanding the mechanism of viral membrane fusion is described.
© 2005 Elsevier Inc. All rights reserved.

Contents

The paramyxoviruses are the etiological agents of many biologically and economically important diseases of man and other animals and the *Paramyxoviridae* includes parainfluenza virus 5 (PIV5) (formerly known as SV5), mumps virus, human parainfluenza virus type 2 (hPIV2) and type 4 (hPIV4), Sendai virus, hPIV1, hPIV3, Newcastle disease virus, measles virus, canine distemper virus, rinderpest virus, respiratory syncytial (RS) virus and the newly emergent highly pathogenic Hendra and Nipah viruses. Two viral glycoproteins are key to the

---

* Corresponding author. Department of Biochemistry, Molecular Biology and Cell Biology, Northwestern University, 2205 Tech Drive, Evanston, IL 60208-3500, USA. Fax: +1 847 491 2467.
E-mail address: ralamb@northwestern.edu (R.A. Lamb).

infection process—an attachment protein that varies across viral families and the fusion (F) protein, which is found in all paramyxoviruses. For many of the paramyxoviruses (NDV, PIVs 1–5 and others), the attachment protein is the hemagglutinin/neuraminidase (HN) protein, but the morbilliviruses, such as measles virus, carry a hemagglutinin (H) protein in place of HN, while the pneumoviruses (RSV) and henipaviruses (Nipah and Hendra) express a distinct attachment glycoprotein (G).

Class I viral fusion proteins

Many viruses, such as influenza viruses, paramyxoviruses, human immunodeficiency virus, herpes viruses and dengue fever virus are enveloped in a lipid membrane and to replicate, these viruses must enter a cell by fusing their own membrane coat with that of the cell. Fusion is caused by viral glycoproteins that are inserted in the viral membrane. The paramyxovirus F proteins belong to the class I viral fusion protein type, of which the best characterized member is the influenza virus hemagglutinin (HA), but which also includes the fusion proteins from retroviruses, coronaviruses, Ebola virus and others (Colman and Lawrence, 2003; Dutch et al., 2000; Earp et al., 2005; Jardetzky and Lamb, 2004). Models for Class I viral fusion protein-mediated membrane merger have been developed primarily from the structural studies of HA (Skehel and Wiley, 2000). In general, class I viral fusion proteins follow the following paradigm. Three identical polypeptide chains assemble into trimers, which are subsequently proteolytically cleaved into two fragments at a specific site N-terminal to an internal hydrophobic domain of approximately 25 amino acids, commonly referred to as the fusion peptide (Fig. 1A). Sequences adjacent to the fusion peptide and the transmembrane (TM) anchor domain typically reveal a 4–3 (heptad) pattern of hydrophobic repeats and are designated HRA and HRB, respectively.

Core trimers of class I viral fusion proteins

Biophysical data indicated that HRA and HRB form a complex and crystallographic studies have shown that HRA and HRB form a helical hairpin or 6-helix bundle structure (core trimer) that is related to that observed for the low-pH-induced proteolytic fragment of HA. For example, the core trimers of PIV5 and hRSV F (Baker et al., 1999; Zhao et al., 2000), HIV gp41 (Caffrey et al., 1998; Chan et al., 1997; Tan et al., 1997; Weissenhorn et al., 1997), Moloney murine leukemia virus envelope protein (Fass et al., 1996), Ebola GP2 (Malashkevich et al., 1999; Weissenhorn et al., 1998) and HTLV-1 (Kobe et al., 1999) fusion proteins all share this similarity in structure (Fig. 1B). While the structural details vary, all reveal a trimeric, coiled-coil beginning near the C-terminal end of the hydrophobic fusion peptide. The C-terminal segment abutting the TM domain is also often helical and packs in an antiparallel direction along the outside of the N-terminal coiled-coil, placing the fusion peptides and TM anchors at the same end of a rod-like structure. These 6-helix bundles (6HB) typically represent a relatively small fraction of the intact fusion protein, yet their structures are generally highly thermostable, with melting
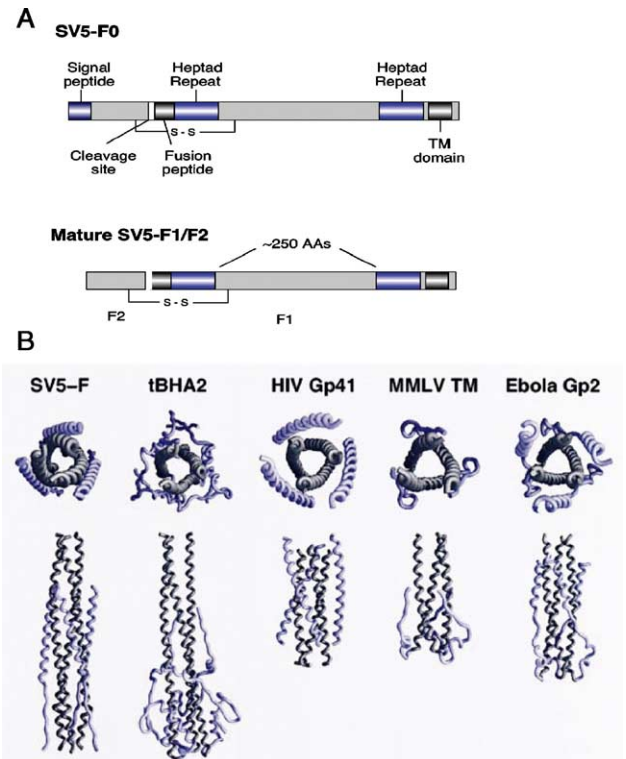

Fig. 1. The paramyxovirus fusion protein and class I fusion protein core trimers. (A) Cleavage activation of a prototypical paramyxovirus F protein from parainfluenza virus 5 (PIV5). The position of the signal sequence, the TM domain, the cleavage site, the hydrophobic fusion peptide and the heptad repeats A and B are indicated. 252 amino acid residues separate the two heptad repeats. (B) Similar hairpin structures are formed by fragments of the membrane-anchored polypeptides of the fusion proteins from different viruses. (Modified from Baker et al., 1999.)

temperatures near 100 °C. Intermediates along the pathway of membrane fusion can be trapped by the addition of peptides derived from either the N-terminal (HRA) or C-terminal (HRB) heptad repeat regions for many class I fusion proteins (Earp et al., 2005; Eckert and Kim, 2001; Fass, 2003), indicating that the intact protein undergoes conformational changes that expose both HR regions, prior to refolding to the final 6HB. The intermediates are thought to represent partially refolded forms of the fusion protein, with a hydrophobic fusion peptide anchored in the target cell membrane and the TM domains anchored to the viral membrane. The formation of the 6HB is tightly linked to the merger of lipid bilayers, and is thought likely to couple the free energy released on protein refolding to membrane fusion (Melikyan et al., 2000; Russell et al., 2001).

Fusion triggering

The triggering event that initiates membrane fusion by different viruses varies substantially for different viral fusion proteins. For influenza virus, membrane fusion occurs upon exposure to the low pH environment of the endosome (Bullough et al., 1994; reviewed in Hernandez et al., 1996), while HIV entry into cells is triggered by binding to the cell-surface proteins CD4 in conjunction with one of the chemokine receptor family members (Damico et al., 1998; Furuta et al., 1998; Hernandez et

al., 1997; Moore et al., 1990). For the paramyxoviruses, membrane fusion occurs at neutral pH, but the trigger mechanism for viral entry remains to be elucidated, although most likely it involves specific interactions with the attachment protein (HN, H or G) (reviewed in Lamb, 1993; Lamb and Kolakofsky, 2001).

Protein refolding and membrane fusion

The general mechanism for class I viral fusion proteins posits the folding of the uncleaved protein to a metastable state, which can be activated to undergo large conformational changes to a more stable fusogenic or post-fusion state. For the influenza HA protein, crystal structures of three forms of the protein have been determined which support this model and provide the structural basis for the general class I mechanism (Bullough et al., 1994; Chen et al., 1998, 1999; Wilson et al., 1981). Influenza HA structures have been determined for the uncleaved (HA0) form (Chen et al., 1998), the cleaved/activated form (HA1/HA2) (Wilson et al., 1981) and the post-fusion form activated by low pH or revealed by the recombinant expression of the C-terminal HA2 fragment (Bullough et al., 1994; Chen et al., 1999). Minor conformational changes are observed between the HA0 and HA1/HA2 structures, which reveal the fusion peptide, initially at the protein surface in HA0, tucked into the interior of the HA2 coiled-coil after proteolysis. The low-pH-induced, post-fusion form shows a dramatic refolding of the HA2 fragment, bringing the fusion peptide and TM anchors into close proximity. For HA, it is thought that proteolytic cleavage primes the protein for membrane fusion (Skehel and Wiley, 2000), potentially influencing the stability of the pre-fusion state. Thus, the attainment of the pre-fusion conformation, its regulation and relative free energy as compared to the post-fusion form are all key to the process by which class I viral fusion proteins function.

Paramyxovirus fusion: capture of intermediates of fusion

To understand the conformations of the F protein from its pre-fusion state through to the post-fusion state, it is necessary to understand the mechanism of activation of F from the metastable state. It was shown that the isolated peptides, called N-1 and C-1, that correspond to the F protein heptad repeats (HRA and HRB, respectively), inhibit fusion (Baker et al., 1999; Joshi et al., 1998). These peptides were then used as tools to dissect the steps in F protein activation from a metastable state (Russell et al., 2001). Both thermal energy and receptor binding by the homotypic HN were found to contribute to F activation (Fig. 2). The N-1 peptide inhibited fusion at an earlier stage (cells incubated at 4 °C) than the C-1 peptide (inhibits only after warming cells to 37 °C), strongly suggesting that the site to which N-1 binds in the F protein is available before the site to which the C-1 peptide binds and that generation of the site to which C-1 binds requires thermal energy (Fig. 2). However, when HA was used as the binding protein in place of HN, even though fusion takes place (albeit less efficiently than when HN is coexpressed), N-1 does not inhibit fusion at 4 °C unlike when HN is used as the binding
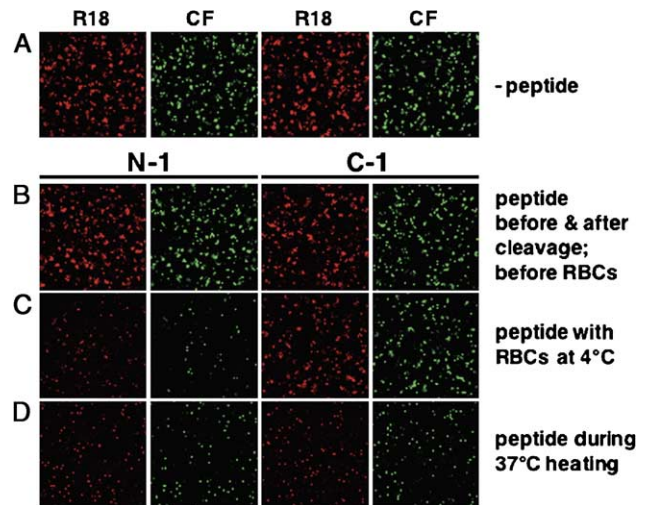

Fig. 2. The N-1 and C-1 peptides inhibit fusion in a temporal manner. CV-1 cells coexpressing PIV5 HN and F protein (FR3) mutated at the cleavage site to prevent intracellular cleavage, were incubated with TPCK-trypsin for 1 h to cleave the F_0 precursor to the F_1 and F_2 subunits. RBCs colabeled with octadecyl rhodamine (R18) (red) and carboxyfluorescein (CF) (green) were bound to the CV-1 cells at 4 °C for 1 h. The samples were incubated at 37 °C for 10 min, reincubated at 4 °C and analyzed for dye transfer by confocal microscopy. Either the N-1 or C-1 peptides were incubated with the samples at the following stages of the assay: (A) no peptide at any stage; (B) peptide before and after cleavage; (C) peptide during RBC binding at 4 °C and (D) peptide during the 37 °C incubation. The samples were washed three times with PBS between each stage. The peptide concentrations were 40 μM. (From Russell et al., 2001 with permission.)

protein but N-1 inhibition does occur on warming the cells to 37 °C. These data strongly suggest that the role of HN is more complex than the mere binding of receptor and indicates that even at 4 °C, HN binding to receptor causes a conformational change in the F protein. In the absence of HN, the conformational change in F can be induced by heating. By using a tagged C-1 peptide, it was shown that the peptide bound to F, and inhibited an intermediate of F that existed until a point preceding membrane merger (Russell et al., 2001). Membrane-incorporated lipids can promote or inhibit fusion in a manner that correlates with their dynamic molecular shapes by either favoring or preventing formation of membrane stalk intermediates of fusion (Chernomordik et al., 1997). F protein-mediated fusion was reversibly arrested by addition of the membrane-binding lipid stearoyl-lysophosphatidylcholine (LPC), which has been shown to inhibit fusion at the point of membrane merger (Chernomordik et al., 1998). By using a temporal order of addition experiment, evidence was obtained indicating that the proteins actively drive membrane fusion by coupling irreversible protein refolding (forming the 6HB) to membrane juxtaposition (Russell et al., 2001). Related data from studies on HIV gp120/gp41 (Melikyan et al., 2000) led to very similar conclusions.

A dual-functional F protein regulatory switch segment: activation and membrane fusion

An unanticipated glimpse of F protein activation came from an examination of the PIV5 6HB (Baker et al., 1999). There is
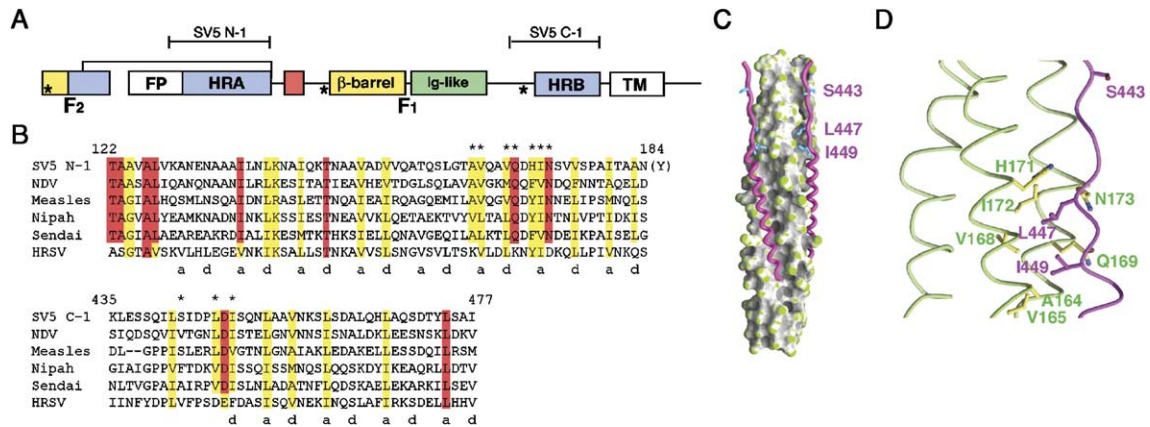
Fig. 3. Mutants in the PIV5 C-1 extended chain region that pack into the core trimer have little effect on 6-helix bundle stability but have dramatic effects on fusion activation. (A) Schematic diagram of the paramyxovirus fusion (F) protein. The positions of the fusion peptide (FP), HRA (residues 129–184), β-barrel domain (β-barrel), immunoglobin-like domain (Ig-like), HRB (residues 449–477) and TM domain are shown. The locations of the N-1 and C-1 peptides from PIV5 F are indicated. The asterisks denote PIV5 residues P22 and P443 and the NDV mutant L289A which have been implicated previously in HN-independent fusion. (Ito et al., 2000; Paterson et al., 2000; Sergel et al., 2000) (B) Sequence alignment of the N-1 and C-1 peptides derived from PIV5 F with the corresponding residues of F proteins from other paramyxovirus genera. HRSV, human respiratory syncytial virus. The asterisks denote the PIV5 N-1 cavity residues, the C-1 cavity-binding residues L447 and I449 and residue 443 that has a hyperactive fusion phenotype when mutated to a proline residue. (C) High-resolution structure of the PIV5 6-helix bundle (6HB) (Baker et al., 1999). The core N-1 trimer is depicted in a surface representation colored by surface curvature and the antiparallel C-1 monomers are depicted by coil representations (magenta). (D) The packing of L447 and I449 into the hydrophobic N-1 cavity. Three N-1 (green) and one C-1 (magenta) chains are depicted by coil representations. (From Russell et al., 2003 with permission.)

a prominent cavity in the HRA trimeric coiled-coil into which HRB side chains L447 and I449 pack tightly (Fig. 3). Mutation of these HRB residues to aromatic residues had little effect on bundle formation as trimers (measured by analytical ultracentrifugation) or stability (as measured by circular dichroism and thermal melting). Surprisingly, when these mutations were introduced into an intact F protein and fusion assayed in cells, a profound effect on F protein activation was found: furthermore, these mutants were hyperactive in fusion. The data indicate that the residues adjacent to HRB regulate the stabilization and activation of pre-fusion metastable F. The data are consistent with this linear segment having dual interaction sites in F, one

in metastable F and one in the 6HB, thereby providing key regulation of the switch between the metastable and fusion-active forms of F (Russell et al., 2003). These data play a very important role in the interpretation of the atomic structure of the intact uncleaved paramyxovirus F protein (see below).

A model for paramyxovirus-mediated fusion

The cascade of paramyxovirus F protein conformational changes that take place while mediating membrane fusion is illustrated in Fig. 4: native structure (which is in a metastable conformation), a temperature-arrested intermediate (which
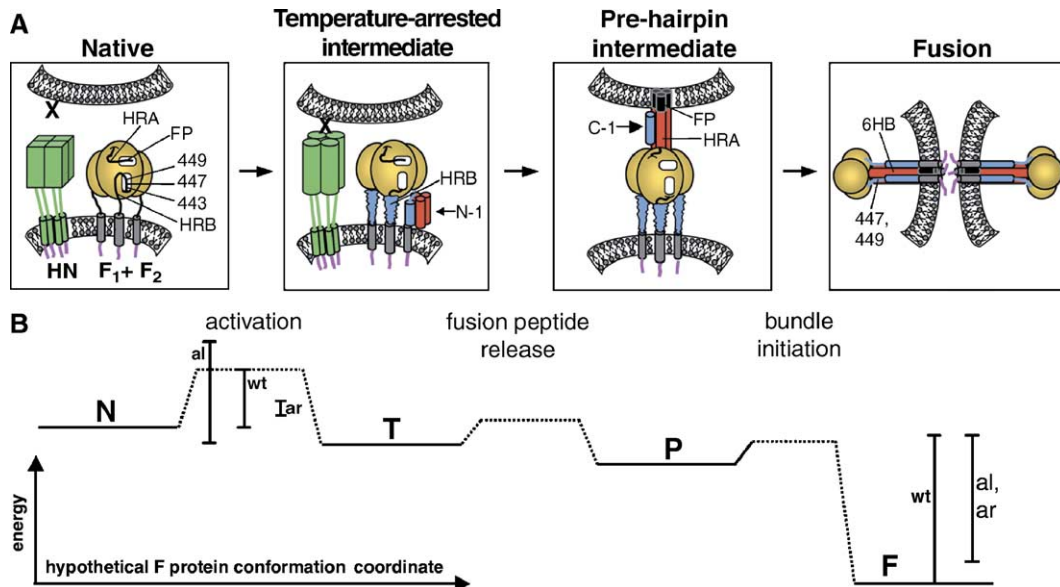

Fig. 4. Model showing the steps for paramyxovirus F protein fusion conformation changes causing virus–cell fusion. See text for a full description. (From Russell et al., 2003 with permission.)

forms after HN binds its receptor at non-fusion permissive temperatures and is susceptible to N-1 binding), a pre-hairpin intermediate (which adheres to target cells independent of HN and is susceptible to C-1 binding) and the post-fusion (sometimes called the Fusogenic) form of F (its formation couples 6HB formation to membrane merger). The experimental data discussed above are consistent with residues 447 and 449 having distinct interaction sites on the F protein, one in the native structure and the other in the cavity formed by HRA trimers in the 6HB of the post-fusion form. The strong correlation between 6HB stability and C-peptide inhibitory potency (Russell et al., 2003) and the coincidence of C-1 inhibition and F protein binding in a previous study (Russell et al., 2001) show that C-1 inhibits membrane fusion by binding to transiently exposed HRA triple-stranded coiled-coils in the pre-hairpin intermediate. Biophysical studies on the N-1/C-peptide mutants show that the aliphatic (al) and aromatic (ar) mutations at L447 and I449 decrease the amount of energy released by mutant 6HB formation; whereas, functional studies on the F mutants are consistent with the aromatic (ar) mutations decreasing and the aliphatic (al) mutations increasing the activation energy barrier of the native state. The hyperactive fusion phenotype of the aromatic mutants is consistent with the facile activation (and subsequent inactivation in the absence of a fusion target) of these F mutants overcompensating for the decrease in energy released by mutant 6HB formation.

Atomic structure of the uncleaved ectodomain of the hPIV3 F protein

A partially proteolyzed structure of a soluble form of the Newcastle disease virus (NDV) F protein was obtained (Chen et al., 2001), revealing the fold of much of the extracellular region of F, forming a trimer, with distinct head, neck and stalk regions, but raising many questions regarding the conformational state of the protein and its relationship to postulated pre-fusion and post-fusion forms. Working on the assumption that all paramyxovirus F proteins mediate fusion by a common mechanism and that the different F proteins will have a closely related structure, given the conservation of cysteine and proline residues among all paramyxovirus F protein sequences, we decided to take a 'genomics' approach and we expressed, purified and attempted to crystallize the uncleaved F protein of nine different paramyxoviruses. To date, the best data came from hPIV3 F. The hPIV3 F protein was expressed in insect cells using the baculovirus system after appending a secretion signal sequence to the mature N-terminus and truncating the protein just prior to the membrane anchor domain (solF0). We crystallized hPIV3 solF0 and single crystals were analyzed by SDS-PAGE to test for potential degradation, as was observed in the crystallization of the NDV F protein (Chen et al., 2001). For hPIV3 solF0, only the intact protein was observed (Yin et al., 2005). The atomic structure of hPIV3 solF0 was solved to 3.05 Å by molecular replacement using as a model a fragment of the NDV F structure (Yin et al., 2005). The hPIV3 F forms a trimer, with distinct head, neck and stalk regions (Fig. 5). The only part of the structure lacking electron density is the fusion peptide and
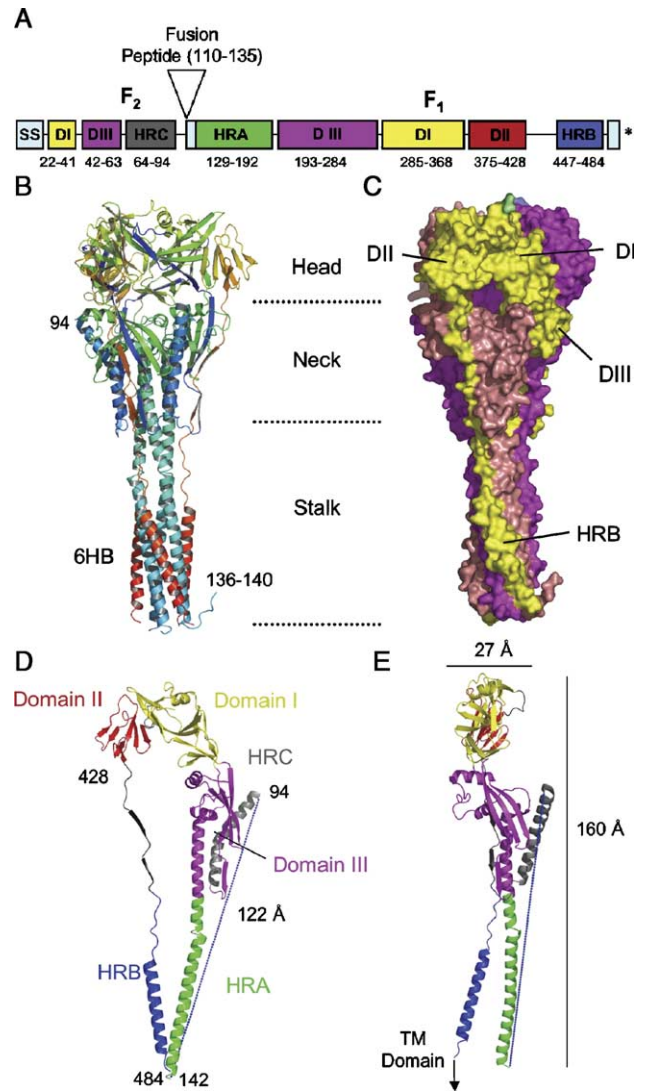

Fig. 5. Structure of the hPIV3 solF0 protein. (A) Schematic of the domain structure of the hPIV3 solF0 protein. Domain regions are indicated with hPIV3 sequence numbers shown below and with colors corresponding to those used in Figs. 1B, D and E. (B) Ribbon diagram of the hPIV3 solF0 trimer. The three chains are colored similarly from blue (N-terminus) to red (C-terminus). Residues 95–135 are disordered in all chains. Residue 94 is labeled in one chain and residues 136–140 at the base of the stalk are ordered in one chain due to crystal packing interactions. (C) Surface representation of the solF0 trimer. Each chain is a different color and Domains I–III and HRB for one chain (yellow) are indicated by the DI, DII, DIII and HRB labels. One radial channel is readily apparent below Domain I and II of the yellow chain and above Domain III of the red chain. (D) Ribbon diagram of the solF0 protein monomer colored by domain. The direct distance within one monomer between residue 94 at the end of HRC and residue 142 at the base of the stalk region is 122 Å. (E) Ribbon diagram of the monomer rotated by 90°, indicating the width and height of the solF0 monomer. An arrow at the C-terminus of the HRB segment points towards the likely position of the transmembrane anchor domain that would be present in the full-length protein. (From Yin et al., 2005 with permission.)

cleavage site, but these residues would be draped flexibly on the exterior of the stalk region. Given that the uncleaved F protein was crystallized, it was unexpected that the structure contains a 6-helix bundle (Fig. 5) that is thought to represent the post-fusion conformation of the protein. Many lines of evidence suggest that the observed conformation primarily represents the

post-fusion form, although the polypeptide chains are intact in the crystal and the fusion peptide is not located at the appropriate end of the 6HB. The 6HB appears to be well formed and undistorted, similar to the previously determined PIV5 and hRSV F 6HB structures (Baker et al., 1999; Zhao et al., 2000). The hPIV3 structure appears to be inconsistent with peptide inhibition data that show, at least for PIV5 F, that the HRA and HRB peptides are exposed at distinct steps of the membrane fusion reaction (Russell et al., 2001 and see Fig. 2). In the current structure, the release of HRB from 6HB would simultaneously expose HRA sites to inhibition, which conflicts with the peptide inhibition data. Instead, the hPIV3 structure would predict that both HRA and HRB peptides would acquire the ability to inhibit membrane fusion simultaneously, requiring the observed 6HB to dissociate in order to be consistent with the previous mechanistic studies. From the current structure, it is also not clear how membrane fusion could be achieved. Cleavage of the hPIV3 solF0 protein would appear to simply allow repositioning of the fusion peptide to the N-terminus of the HRA coiled-coil, and concomitant insertion into the anchoring membrane for the TM domain. Finally, the current structure cannot explain the behavior of F protein mutants that destabilize the pre-fusion conformation of F and significantly enhance its membrane fusion activity (Colman and Lawrence, 2003; Paterson et al., 2000; Russell et al., 2003) (see Figs. 3–5). Mutation of two hydrophobic residues of HRB in PIV5 (447 and 449 in PIV5 corresponding to 454 and 456 in hPIV3) to larger aromatic residues, leads to a hyper-fusion phenotype of the PIV5 F protein, which is most easily interpreted as leading to a destabilization of the pre-fusion conformation (Russell et al., 2003). The mutation of conserved glycine residues in the fusion peptide leads to similar behavior (Russell et al., 2004).

The structure of hPIV3 solF0 (Fig. 5) also raises questions regarding the formation and stability of the pre-fusion conformation of the paramyxovirus F protein. If the soluble, secreted hPIV3 and NDV F proteins, and by inference other paramyxovirus family members as well, primarily adopt a post-fusion conformation, there are at least two possible explanations for this behavior. First, the TM anchor (and potentially the cytoplasmic tail; Waning et al., 2004) could be an important determinant of the stability of the pre-fusion conformation, providing a significant fraction of the energy barrier that traps the protein in a metastable state. In this case, the secreted protein may fold to the pre-fusion form transiently, but then refold to the post-fusion form. A second possible explanation for the structural results is that the TM domain is important for the protein to attain the pre-fusion metastable state and that in the absence of this region, the soluble F protein folds directly to the final, most stable post-fusion conformation. In either case, it appears that the amino acids comprising the intact F protein ectodomain are not sufficient for the protein to fold to and maintain a metastable conformation.

Atomic structure of HN and the role(s) of HN in fusion activation

A large body of data supports the view that HN promotes fusion by the paramyxovirus virus F protein (reviewed in Lamb and Kolakofsky, 2001). It is now generally thought that F with the homotypic HN (H or G) protein has to be expressed in the same cell and biochemical data indicate that F and HN coassociate (reviewed in Morrison, 2003). Thus, knowledge of the atomic structure of HN may help to understand HN activation of F for membrane fusion. To date, the atomic
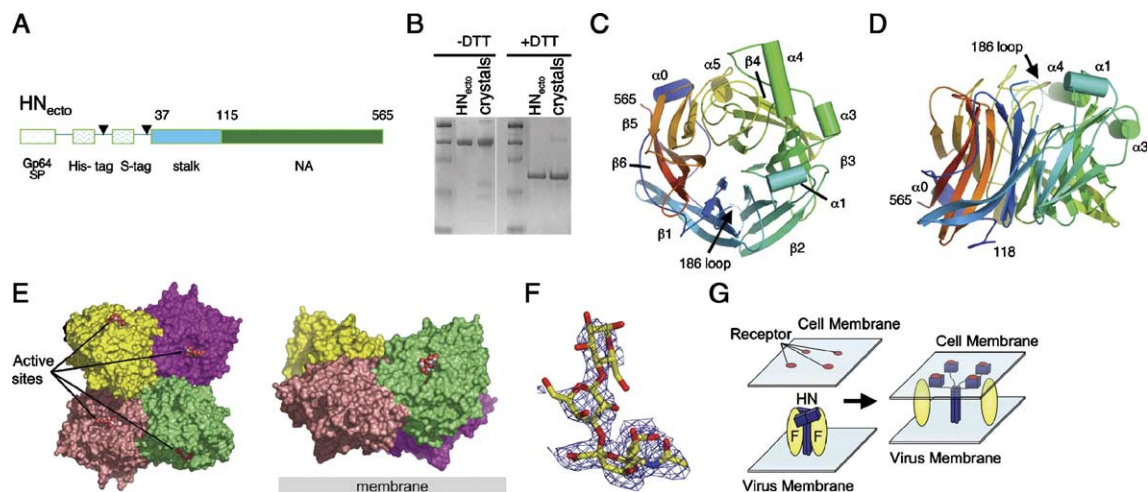

Fig. 6. Atomic structure of the PIV5 hemagglutinin-neuraminidase at 2.6 Å resolution. (A) Construct for expression of HN^{ecto} in insect cells. Downward arrows correspond to protease cleavage sites in the pBacgus-3 vector. (B) SDS-PAGE analysis of HN$_{ecto}$ and dissolved HN$_{ecto}$ crystals under reducing and non-reducing conditions. (C and D) Schematic cartoon showing top and side view of PIV5 HN. Helices are shown in cylinders and β-strands in arrowed belts. The N-terminus is shown in blue and the C-terminus in red. The missing loop from residues 186 to 190 is indicated as dashed blue lines. (E) PIV5 HN tetramers. Active sites are marked by space filling representations of the ligand, sialyllactose. The four subunits are shown in different colors. (Left) Top view of the PIV5 HN tetramer arrangement; (Right) side view of PIV5 HN tetramer arrangement, with a 60° packing angle between dimers. (F) Electron density observed for α2,3-sialyllactose soaked crystal at 2.5 Å resolution. (G) A model for HN tetramer rearrangement upon cell-surface receptor binding. The HN tetramer is primarily stabilized by the N-terminal stalk region and can interact with F protein. Sialic acid receptors are displayed at the cell surface, where binding of the individual HN head (neuraminidase active; NA) domains could perturb the NA tetramer arrangement, consistent with the weak interactions between NA domains. Changes in the HN NA domain tetramer could affect interactions and trigger membrane fusion. (From Yuan et al., 2005 with permission.)

structure of the HN protein of NDV (Crennell et al., 2000; Zaitsev et al., 2004), hPIV3 (Lawrence et al., 2004) and PIV5 (Yuan et al., 2005) has been determined.

For PIV5 HN, the entire HN ectodomain (HN$_{ecto}$), residues 37–565, was expressed in insect cells from recombinant baculoviruses (Fig. 6A). Secreted HN protein was purified to homogeneity by using Co^{2+} affinity chromatography and gel filtration chromatography. HN$_{ecto}$ elutes from a gel filtration column with a $M_r \sim 265$ kDa, which is very close to the predicted mass of the tetramer (250–260 kDa). On non-reducing SDS-PAGE, HN$_{ecto}$ migrates at the size expected for a disulfide-linked dimer (Fig. 6B). These observations indicate that HN$_{ecto}$ forms disulfide-linked dimers through C111 and the dimers associate into tetramers in solution, consistent with previous studies of the HN oligomeric arrangement (Ng et al., 1989, 1990). The formation of a stable HN tetramer in solution requires the N-terminal stalk region of the protein. PIV5 HN$_{ecto}$ was crystallized and the structure was determined by molecular replacement using NDV HN as a model (Figs. 6C and D). The structures of HN$_{ecto}$ with sialic acid, the inhibitor DANA and with sialyllactose were also determined (Yuan et al., 2005).

The salient results from the structural studies on PIV5 HN (Yuan et al., 2005) are as follows. (1) The HN receptor sialyllactose was found in an intact form at pH 8.0 and the sialic acid moiety exists in a distorted conformation induced by interactions with HN. (2) The HN ectodomain exists as a tetramer in solution and the presence of the stalk region is critical for the formation of the stable tetramer. However, in the HN$_{ecto}$ crystal structure, even though the protein is intact (Fig. 6), the stalk region was not visible in the electron density suggesting the linker region between the stalk and NA domains is flexible. (3) The PIV5 HN contains only one sialic binding site unlike for NDV that contains two sialic binding sites, the catalytic site and a second site formed by the juxtaposition of two monomers (Zaitsev et al., 2004). However, for PIV5, HN not only was a second sialic acid molecule not observed but the PIV5 HN molecule could also not form the second sialic acid binding site between two monomers due to changes in sequence and conformation. (4) The PIV5 HN sialic acid-binding active site, like that of hPIV3 HN (Lawrence et al., 2004), does not undergo conformational change on binding ligand, unlike those proposed for NDV HN where ligand binding to the catalytic site is proposed to influence the oligomeric arrangement of NDV HN and create the second sialic acid binding site (Crennell et al., 2000; Zaitsev et al., 2004). Based on the second sialic acid binding site in NDV HN, Zaitsev et al. (2004) proposed a model for HN activating F for fusion.

For PIV5, an alternative model for HN involvement in membrane fusion was proposed that is consistent with the available data and that involves ligand-dependent changes in the HN oligomer that are driven by surface:surface interactions (Fig. 6) (Yuan et al., 2005). In this model, the HN dimer/tetramer forms in the absence of ligands and can interact with the F protein, potentially through lateral interactions on two sides of the tetramer. Engagement of cell surface receptors could trigger the partial disassembly of the HN tetramer, assuming that the energy of binding of the individual HN sites to distinct sialic receptors is sufficient to perturb the weak NA domain interactions. Opening of the tetrameric head, driven by the energy of receptor engagement, could lead to changes in both the HN stalk region (the HN stalk domain is thought to interact with F) (reviewed in Colman and Lawrence, 2003) and the interaction with F, thus activating F for membrane fusion.

Conclusions

In the last 5 years, atomic structures of F and HN proteins of paramyxoviruses have brought new knowledge towards understanding the mechanism of viral membrane fusion. However, a great deal more information is needed. The key studies needed for understanding paramyxovirus-mediated membrane fusion are: (1) obtaining the structure of the uncleaved metastable form of F; (2) understanding the conformation of the metastable cleaved F protein; (3) learning how HN protein activates fusion and (4) studying the interactions between F and HN. These mechanistic studies require both structural information and biochemical experiments if a complete understanding of fusion is to be obtained.

Acknowledgments

References

Baker, K.A., Dutch, R.E., Lamb, R.A., Jardetzky, T.S., 1999. Structural basis for paramyxovirus-mediated membrane fusion. Mol. Cell 3, 309–319.

Bullough, P.A., Hughson, F.M., Skehel, J.J., Wiley, D.C., 1994. Structure of influenza haemagglutinin at the pH of membrane fusion. Nature 371, 37–43.

Caffrey, M., Cai, M., Kaufman, J., Stahl, S.J., Gronenborn, A.M., Clore, G.M., 1998. Three-dimensional solution structure of the 44 kDa ectodomain of SIV gp41. EMBO J. 17, 4572–4584.

Chan, D.C., Fass, D., Berger, J.M., Kim, P.S., 1997. Core structure of gp41 from the HIV envelope glycoprotein. Cell 89, 263–273.

Chen, J., Lee, K.H., Steinhauer, D.A., Stevens, D.J., Skehel, J.J., Wiley, D.C., 1998. Structure of the hemagglutinin precursor cleavage site, a determinant of influenza pathogenicity and the origin of the labile conformation. Cell 95, 409–417.

Chen, J., Skehel, J.J., Wiley, D.C., 1999. N- and C-terminal residues combine in the fusion-pH influenza hemagglutinin HA2 subunit to form an N cap that terminates the triple-stranded coiled coil. Proc. Natl. Acad. Sci. U.S.A. 96, 8967–8972.

Chen, L., Gorman, J.J., McKimm-Breschkin, J., Lawrence, L.J., Tulloch, P.A., Smith, B.J., Colman, P.M., Lawrence, M.C., 2001. The structure of the fusion glycoprotein of Newcastle disease virus suggests a novel paradigm for the molecular mechanism of membrane fusion. Structure 9, 255–266.

Chernomordik, L.V., Leikina, E., Frolov, V., Bronk, P., Zimmerberg, J., 1997. An early stage of membrane fusion mediated by the low pH conformation of influenza hemagglutinin depends upon membrane lipids. J. Cell Biol. 136, 81–93.

Chernomordik, L.V., Frolov, V.A., Leikina, E., Bronk, P., Zimmerberg, J., 1998. The pathway of membrane fusion catalyzed by influenza hemagglutinin: restriction of lipids, hemifusion, and lipidic fusion pore formation. J. Cell Biol. 140, 1369–1382.

Colman, P.M., Lawrence, M.C., 2003. The structural biology of type I viral membrane fusion. Nat. Rev., Mol. Cell Biol. 4, 309–319.

Crennell, S., Takimoto, T., Portner, A., Taylor, G., 2000. Crystal structure of the multifunctional paramyxovirus hemagglutinin-neuraminidase. Nat. Struct. Biol. 7, 1068–1074.

Damico, R.L., Crane, J., Bates, P., 1998. Receptor-triggered membrane association of a model retroviral glycoprotein. Proc. Natl. Acad. Sci. U.S.A. 95, 2580–2585.

Dutch, R.E., Jardetzky, T.S., Lamb, R.A., 2000. Virus membrane fusion proteins: biological machines that undergo a metamorphosis. Biosci. Rep. 20 (6), 597–612.

Earp, L.J., Delos, S.E., Park, H.E., White, J.M., 2005. The many mechanisms of viral membrane fusion proteins. Curr. Top. Microbiol. Immunol. 285, 25–66.

Eckert, D.M., Kim, P.S., 2001. Mechanisms of viral membrane fusion and its inhibition. Annu. Rev. Biochem. 70, 777–810.

Fass, D., 2003. Conformational changes in enveloped virus surface proteins during cell entry. Adv. Protein Chem. 64, 325–362.

Fass, D., Harrison, S.C., Kim, P.S., 1996. Retrovirus envelope domain at 1.7 Å resolution. Nat. Struct. Biol. 3, 465–469.

Furuta, R.A., Wild, C.T., Weng, Y., Weiss, C.D., 1998. Capture of an early fusion-active conformation of HIV-1 gp41. Nat. Struct. Biol. 5, 276–279.

Hernandez, L.D., Hoffman, L.R., Wolfsberg, T.G., White, J.M., 1996. Virus–cell and cell–cell fusion. Annu. Rev. Cell Dev. Biol. 12, 627–661.

Hernandez, L.D., Peters, R.J., Delos, S.E., Young, J.A.T., Agard, D.A., White, J.M., 1997. Activation of a retroviral membrane fusion protein: soluble receptor-induced liposome binding of the ALSV envelope glycoprotein. J. Cell Biol. 139, 1455–1464.

Ito, M., Nishio, M., Komada, H., Ito, Y., Tsurudome, M., 2000. An amino acid in the heptad repeat 1 domain is important for the haemagglutinin-neuraminidase-independent fusing activity of simian virus 5 fusion protein. J. Gen. Virol. 81, 719–727.

Jardetzky, T.S., Lamb, R.A., 2004. Virology: a class act. Nature 427, 307–308.

Joshi, S.B., Dutch, R.E., Lamb, R.A., 1998. A core trimer of the paramyxovirus fusion protein: parallels to influenza virus hemagglutinin and HIV-1 gp41. Virology 248, 20–34.

Kobe, B., Center, R.J., Kemp, B.E., Poumbourios, P., 1999. Crystal structure of human T cell leukemia virus type 1 gp21 ectodomain crystallized as a maltose-binding protein chimera reveals structural evolution of retroviral transmembrane proteins. Proc. Natl. Acad. Sci. U.S.A. 96, 4319–4324.

Lamb, R.A., 1993. Paramyxovirus fusion: a hypothesis for changes. Virology 197, 1–11.

Lamb, R.A., Kolakofsky, D., 2001. Paramyxoviridae: the viruses and their replication. In: Knipe, D.M., Howley, P.M. (Eds.), Fields Virology, 4th ed. Lippincott, Williams and Wilkins, PA, pp. 1305–1340.

Lawrence, M.C., Borg, N.A., Streltsov, V.A., Pilling, P.A., Epa, V.C., Varghese, J.N., McKimm-Breschkin, J.L., Colman, P.M., 2004. Structure of the haemagglutinin-neuraminidase from human parainfluenza virus type III. J. Mol. Biol. 335, 1343–1357.

Malashkevich, V.N., Schneider, B.J., McNally, M.L., Milhollen, M.A., Pang, J.X., Kim, P.S., 1999. Core structure of the envelope glycoprotein GP2 from Ebola virus at 1.9-A resolution. Proc. Natl. Acad. Sci. U.S.A. 96, 2662–2667.

Melikyan, G.B., Markosyan, R.M., Hemmati, H., Delmedico, M.K., Lambert, D.M., Cohen, F.S., 2000. Evidence that the transition of HIV-1 gp41 into a six-helix bundle, not the bundle configuration, induces membrane fusion. J. Cell Biol. 151, 413–423.

Moore, J.P., McKeating, J.A., Weiss, R.A., Sattentau, Q.J., 1990. Dissociation of gp120 from HIV-1 virions induced by soluble CD4. Science 250, 1130–1142.

Morrison, T.G., 2003. Structure and function of a paramyxovirus fusion protein. Biochim. Biophys. Acta 1614, 73–84.

Ng, D.T., Randall, R.E., Lamb, R.A., 1989. Intracellular maturation and transport of the SV5 type II glycoprotein hemagglutinin-neuraminidase: specific and transient association with GRP78-BiP in the endoplasmic reticulum and extensive internalization from the cell surface. J. Cell Biol. 109, 3273–3289.

Ng, D.T., Hiebert, S.W., Lamb, R.A., 1990. Different roles of individual N-linked oligosaccharide chains in folding, assembly, and transport of the simian virus 5 hemagglutinin-neuraminidase. Mol. Cell. Biol. 10, 1989–2001.

Paterson, R.G., Russell, C.J., Lamb, R.A., 2000. Fusion protein of the paramyxovirus SV5: destabilizing and stabilizing mutants of fusion activation. Virology 270, 17–30.

Russell, C.J., Jardetzky, T.S., Lamb, R.A., 2001. Membrane fusion machines of paramyxoviruses: capture of intermediates of fusion. EMBO J. 20, 4024–4034.

Russell, C.J., Kantor, K.L., Jardetzky, T.S., Lamb, R.A., 2003. A dual-functional paramyxovirus F protein regulatory switch segment: activation and membrane fusion. J. Cell Biol. 163, 363–374.

Russell, C.J., Jardetzky, T.S., Lamb, R.A., 2004. Conserved glycine residues in the fusion peptide of the paramyxovirus fusion protein regulate activation of the native state. J. Virol. 78, 13727–13742.

Sergel, T.A., McGinnes, L.W., Morrison, T.G., 2000. A single amino acid change in the Newcastle disease virus fusion protein alters the requirement for HN protein in fusion. J. Virol. 74, 5101–5107.

Skehel, J.J., Wiley, D.C., 2000. Receptor binding and membrane fusion in virus entry: the influenza hemagglutinin. Annu. Rev. Biochem. 69, 531–569.

Tan, K., Liu, J.-H., Wang, J.-H., Shen, S., Lu, M., 1997. Atomic structure of a thermostable subdomain of HIV-1 gp41. Proc. Natl. Acad. Sci. U.S.A. 94, 12303–12308.

Waning, D.L., Russell, C.J., Jardetzky, T.S., Lamb, R.A., 2004. Activation of a paramyxovirus fusion protein is modulated by inside-out signaling from the cytoplasmic tail. Proc. Natl. Acad. Sci. U.S.A. 101, 9217–9222.

Weissenhorn, W., Calder, L.J., Dessen, A., Laue, T., Skehel, J.J., Wiley, D.C., 1997. Assembly of a rod-shaped chimera of a trimeric GCN4 zipper and the HIV-1 gp41 ectodomain expressed in *Escherichia coli*. Proc. Natl. Acad. Sci. U.S.A. 94, 6065–6069.

Weissenhorn, W., Carfi, A., Lee, K.-H., Skehel, J.J., Wiley, D.C., 1998. Crystal structure of the Ebola virus membrane fusion subunit, GP2, from the envelope glycoprotein ectodomain. Mol. Cell 2, 605–616.

Wilson, I.A., Skehel, J.J., Wiley, D.C., 1981. Structure of the haemagglutinin membrane glycoprotein of influenza virus at 3 Å resolution. Nature 289, 366–375.

Yin, H.-S., Paterson, R.G., Wen, X., Lamb, R.A., Jardetzky, T.S., 2005. Structure of the uncleaved ectodomain of the paramyxovirus (hPIV3) fusion protein. Proc. Natl. Acad. Sci. U.S.A. 102, 9288–9293.

Yuan, P., Thompson, T., Wurzburg, B.A., Paterson, R.G., Lamb, R.A., Jardetzky, T.S., 2005. Structural studies of the parainfluenza virus 5 hemagglutinin-neuraminidase tetramer in complex with its receptor, sialyllactose. Structure 13, 1–13.

Zaitsev, V., Von Itzsteine, M., Groves, D., Kiefel, M., Takimoto, T., Portner, A., Taylor, G., 2004. Second sialic acid binding site in Newcastle disease virus hemagglutinin-neuraminidase: implications in fusion. J. Virol. 78, 3733–3741.

Zhao, X., Singh, M., Malashkevich, V.N., Kim, P.S., 2000. Structural characterization of the human respiratory syncytial virus fusion protein core. Proc. Natl. Acad. Sci. U.S.A. 97, 14172–14177.